[2] Stavsky, Y., "Bending and stretching of laminated aeolotropic plates," Proc. Am. Soc. Civ. Engrs., J. Eng. Mech. Div. **87**, 31–56 (1961).

[3] Newman, M. and Forray, M., "Thermal stresses and deflections in thin plates with temperature-dependent elastic moduli," J. Aerospace Sci. **29**, 372–373 (1962).

Simplification of the Shock-Tube Equation

J. Gordon Hall* and Anthony L. Russo†

Cornell Aeronautical Laboratory Inc., Buffalo, N. Y.

A useful simplification of the shock-tube equation is pointed out for shock Mach numbers exceeding about 3. For given driver gas specific heat ratio, shock-tube performance can be expressed explicitly for all initial conditions (including area change) by a single curve. The two basic variables are the shock strength normalized in terms of diaphragm pressure ratio, and the diaphragm density ratio. Universal performance curves are given in this form. Application to tailored-interface conditions and optimum performance of buffered tubes is described.

The ideal-gas shock-tube equation in terms of shock Mach number M_s and initial conditions before diaphragm rupture is[1]

$$\frac{1}{gP_{41}}\left[\frac{2\gamma_1}{\gamma_1+1}M_s^2-\frac{\gamma_1-1}{\gamma_1+1}\right]=\left[1-\frac{(\gamma_4-1)(M_s^2-1)}{(\gamma_1+1)A_{41}M_s}g^{-(\gamma_4-1)/2\gamma_4}\right]^{2\gamma_4/(\gamma_4-1)} \quad (1)$$

where

M_s = shock speed divided by sound speed a_1 ahead of shock
P_{41} = p_4/p_1 = initial pressure ratio (>1) across diaphragm
A_{41} = a_4/a_1 = initial sound speed ratio across diaphragm
g = parameter accounting for tube cross-section area change at diaphragm
γ = specific heat ratio

Subscripts 4 and 1 denote initial states of driver and driven gases, respectively.

The effect of an area change at the diaphragm can be interpreted in terms of a constant-area shock tube having initial diaphragm pressure ratio gP_{41} and sound-speed ratio $A_{41}g^{(\gamma_4-1)/2\gamma_4}$. Appropriate values of g are given in the literature, e.g., Refs. 1 and 2; g is unity for equal driver and driven-tube areas and has a maximum value of about 2 for infinite contraction ratio.

For given initial conditions of P_{41}, A_{41}, γ_4, γ_1, and g, the solution of Eq. (1) for M_s requires an iterative procedure. Extensive graphical results therefore have been given in previous publications, usually in the form M_s vs P_{41} with A_{41}, γ_4, and γ_1 as independent parameters. A large number of curves thus are required to represent shock tube performance over a range of A_{41} values for usual combinations of γ_4 and γ_1.

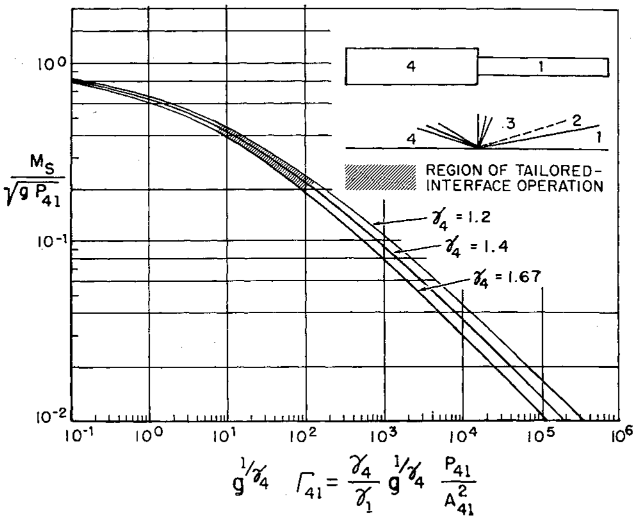

Fig. 1 Normalized shock tube performance; applicable for $M_s \geq 3$ and arbitrary γ_1

The purpose of the present note is to point out that, for M_s exceeding about 3, the approximation of neglecting 1 and $(\gamma_1-1)/2\gamma_1$ compared to M_s^2 enables Eq. (1) to be put into a reduced form that greatly simplifies the interpretation, graphical representation, and determination of shock-tube performance. The reduced form of Eq. (1) is

$$Y=\{1-[(\gamma_4-1)/(2\gamma_4)^{1/2}]YX^{1/2}\}^{\gamma_4/(\gamma_4-1)} \quad (2)$$

where

$$Y=\left(\frac{2\gamma_1}{\gamma_1+1}\right)^{1/2}\frac{M_s}{(gP_{41})^{1/2}} \qquad X=\frac{g^{1/\gamma_4}\Gamma_{41}}{\gamma_1+1}$$

and

$$\Gamma_{41}=\gamma_4P_{41}/\gamma_1A_{41}^2$$

is the initial density ratio across the diaphragm. Thus the reduced equation contains only one independent parameter, γ_4, in addition to the two variables Y and X. The variable Y is the shock Mach number normalized in terms of the diaphragm pressure ratio P_{41}. The variable X is essentially the diaphragm density ratio Γ_{41} and therefore accounts for the effects of both P_{41} and A_{41}.

For practical purposes (to within a few percent accuracy), the plot of shock-tube performance from Eq. (2) can be simplified somewhat further without loss of generality by plotting $M_s/(gP_{41})^{1/2}$ vs $g^{1/\gamma_4}\Gamma_{41}$, i.e., omitting the factors in Y and X involving γ_1. The insensitivity to γ_1 (in the usual range of γ_1) is suggested by the limiting behavior of $M_s/(gP_{41})^{1/2}$ as $\Gamma_{41}\rightarrow 0$ via $A_{41}\rightarrow\infty$, and as $\Gamma_{41}\rightarrow\infty$ via $P_{41}\rightarrow\infty$. Three such plots of tube performance are shown in Fig. 1 for values of γ_4 of 1.67, 1.4, and 1.2. These curves determine M_s in convenient form for arbitrary values of P_{41}, A_{41}, γ_1, and g. It is emphasized that the curves apply only for M_s exceeding about 3.

All the basic aspects of ideal shock-tube performance are made conveniently apparent by this representation. For a given value of γ_4, the normalized performance, i.e., $M_s/(gP_{41})^{1/2}$, depends only on the diaphragm density ratio Γ_{41}. The most efficient operation for production of strong shocks, i.e., maximum M_s for given P_{41}, is at low values of Γ_{41} which are obtained with large values of the sound-speed ratio A_{41}. Some increase in performance [i.e., $M_s/(gP_{41})^{1/2}$] is obtained with decrease in γ_4, but this increase becomes small at lower values of Γ_{41}.

Received by ARS December 10, 1962. This study was done under Contract No. AF 33(657)-8860 for the Aeronautical Research Laboratory, Office of Aerospace Research, U. S. Air Force.

* Assistant Head, Aerodynamic Research Department.
† Research Mechanical Engineer.

γ_4	γ_1	$g^{1/\gamma_4}\,\Gamma_{41}$ FOR TAILORING, SHOCK MACH NO. ~ M_s: 3	5	∞
1.67	1.2	24	46	83
	1.4	13	18	23
	1.67	8	10	12
1.4	1.2	27	53	99
	1.4	13	20	27
	1.67	8	10	13
1.2	1.2	31	70	136
	1.4	15	24	34
	1.67	8	10	13

Fig. 2 Tailored-interface conditions for shock tubes (ideal gases)

The region of tailored-interface operation, where the shock wave reflected from the driven-tube end produces no reflected waves on interacting with the interface, also is shown. For shock waves sufficiently strong that $M_s^2 \gg (\gamma_1 + 1)/(\gamma_1 - 1)$ (i.e., limiting density ratio for ideal gas), tailoring occurs at one point only on the $M_s/(gP_{41})^{1/2}$ vs $g^{1/\gamma_4}\Gamma_{41}$ curve. The range of $g^{1/\gamma_4}\Gamma_{41}$ over which tailoring occurs for $3 \leq M_s \leq \infty$ is quite narrow. Conditions for tailoring are summarized in Fig. 2.

The use of these reduced variables simplifies the analysis of more complex shock-tube configurations. In the case of the buffered shock tube,[3] for example, similar approximations give the result that the final shock Mach number attained for given initial states of the driver and driven gases depends only on the initial driver-buffer gas density ratio. Previous numerical results for the buffered shock tube which show the effects of varying buffer-gas pressure and molecular weight[3] can be correlated conveniently in terms of this density ratio.

References

[1] Glass, I. I. and Hall, J. G., "Shock tubes," *Handbook of Supersonic Aerodynamics*, NAVORD Rept. 1488, Vol. 6, Sec. 18, p. 405 (December 1959).

[2] Alpher, R. A. and White, D. R., "Ideal theory of shock tubes with area change near diaphragm," General Electric Research Lab. Rept. 57-RL-1664 (January 1957).

[3] Russo, A. L. and Hertzberg, A., "A method for improving the performance of shock tubes," Jet Propulsion **27**, 1191–1193 (1957).

Electromagnetic Torques Operating on Satellites Using Snap Reactor Power Systems

J. H. Bick*

North American Aviation Science Center, Canoga Park, Calif.

THE satellites that use Snap nuclear reactor systems for auxiliary power are unique in both the size of the permanent magnet carried and the amount of electric current generated while in orbit. The interaction of the electric and magnetic fields of the satellites with the geomagnetic field will produce torques that may affect the satellite attitude. It is the purpose of this note to express these electromagnetic torques as a function of time in order that they may be used as an inhomogeneous forcing function in the dynamic attitude control equations.

Received December 26, 1962.

* Member of the Technical Staff.

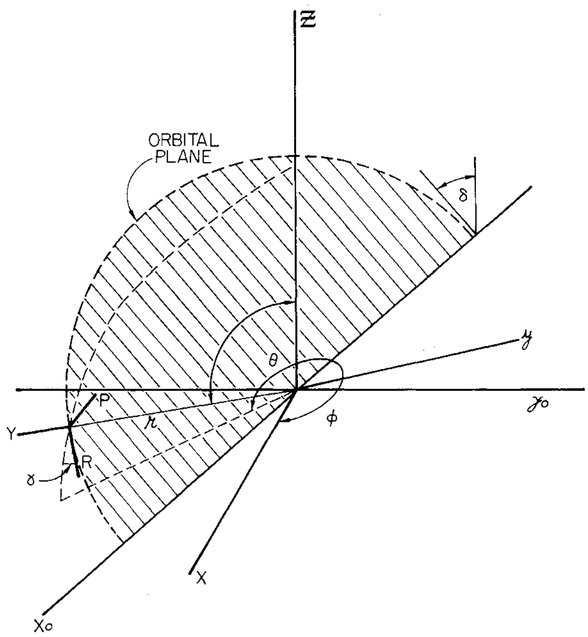

Fig. 1 Coordinate system used in torque analysis

The geomagnetic field may be derived from a potential, $V(r,\theta,\varphi)$ expressed in powers of orbit radius and normalized associated Legendre polynomials.[1] The components of the field at the location of the satellite are

$$B_r = \partial V/\partial r \tag{1}$$

$$B_\theta = (1/r)(\partial V/\partial \theta) \tag{2}$$

$$B_\varphi = -(1/r \sin\theta)(\partial V/\partial \varphi) \tag{3}$$

where r, θ, and φ are conventional spherical coordinates centered in the earth, θ being measured from the North Pole. The more terms taken in the series expansions for the field components, the higher the degree of accuracy that will be obtained. The magnetic moment of the satellite has components in the roll, pitch, and yaw directions, where the yaw axis is parallel to the local vertical, the roll axis is in the orbital plane and perpendicular to the yaw, and the pitch axis forms the third axis of a right-handed Cartesian set, permuted in the order roll, pitch, yaw (see Fig. 1). Note that, if the orbital plane contains the line connecting the geographic poles, the roll, yaw, and pitch components of the satellite magnetic moment vector are, respectively, parallel to B_θ, B_r, and B_φ.

The perturbing torque is the vector product of the satellite and geomagnetic fields. If one lets γ be the positive angle measured from the positive roll axis to the tangent to the circle, r = const at the satellite (see Fig. 1), and defines the components of the satellite field as M_R, M_P, and M_Y along the roll, pitch, and yaw axes, then the torque components about these axes are

$$T_R = M_Y(B_\varphi \cos\gamma - B_\theta \sin\gamma) - M_P B_r \tag{4}$$

$$T_P = M_R B_r - M_Y(B_\varphi \cos\gamma - B_\theta \sin\gamma) \tag{5}$$

$$T_Y = M_P(B_\theta \cos\gamma + B_\varphi \sin\gamma) - M_R(B_\varphi \cos\gamma - B_\theta \sin\gamma) \tag{6}$$

expressed in the roll, pitch, yaw coordinate system.

Having found the components of the torque vector, it is necessary to express the orbital radius and the angles γ, θ, and

[1] Johnson, F. S., *Satellite Environment Handbook* (Stanford University Press, Stanford, Calif., 1961), p. 127.